Mixing processes at an ice-covered river confluence

Pascale M. Biron[1,*], *Thomas* Buffin-Bélanger[2], and *Nancy* Martel[2]

[1]Department of Geography, Planning and Envirronment, Concordia University, 1455 De Maisonneuve Blvd W., Montreal, Quebec, H3G 1M8, Canada
[2]Département de biologie, chimie et géographie, Université du Québec à Rimouski, 300 allée des Ursulines, Rimouski, Quebec, G5L 3A1, Canada

Abstract. River confluences are characterized by a complex mixing zone with three-dimensional turbulent structures, which can be affected by the presence of an ice cover during the winter. The objective of this study is to characterize the flow structure in the mixing zone at a medium-size (~ 40 m) river confluence with and without an ice cover. Detailed velocity profiles were collected under the ice along the mixing plane with an Acoustic Doppler Velocimeter. For the ice-free conditions, drone imagery was used to characterize the mixing layer structures for various flow stages. Results indicate that during the ice-free conditions, very large Kelvin-Helmholtz (KH) coherent structures are visible due to turbidity differences, and occupy up to 50% of the width of the parent channel. During winter, the ice cover affects velocity profiles by moving the highest velocities towards the center of the profiles. Large turbulent structures are visible in both the streamwise and lateral velocity components. The strong correlation between these velocity components indicates that KH vortices are the dominating coherent structures in the mixing zone. A spatio-temporal conceptual model is presented to illustrate the main differences on the three-dimensional flow structure at the river confluence with and without the ice cover.

1. Introduction

River confluences are characterized by a complex mixing zone with three-dimensional turbulent structures. The position of the mixing interface and the type of flow structures are influenced by the junction angle, the discharge ratio (Qr), the momentum flux ratio (Mr) and the bed morphology, in particular bed discordance [1-4]. Several conceptual models have been proposed to describe flow structure at these sites since the original work of Best (1987) [1]. Some have highlighted the importance of streamwise-oriented structures (SOV) [3,5] whereas others have focused on the distortion of vertical Kelvin-Helmholtz (KH) vortices induced by bed discordance [4,6]. Whilst there is still no clear consensus on the role of these various structures, there is an agreement that vortices in the mixing zone can play a significant role in sediment transport [4,5,7] and hence on the morphological evolution of the confluence.

* Corresponding author: pascale.biron@concordia.ca

The majority of studies on confluences were conducted in small laboratory flumes or in small natural channels, although large confluences have also received attention in the last decade [8]. There remains an overall paucity of studies on medium-sized confluences (30-50 m in width) to help develop general models of mixing processes that are not scale dependent.

In cold regions where an ice cover is present for most of the winter period, mixing processes are also likely affected by the roughness effect of the ice whilst the ice cover formation can also be affected by flow structure at the confluence. However, very few studies have examined the impact of an ice cover on the flow structure at a confluence. In simple channels, the hypothesis is that two independent flow layers, one associated with the bed and one with the ice-water interface, result in two opposite logarithmic profiles, with maximum velocities occurring around mid depth [9]. In meandering rivers, two stacked counter-rotating helical flow cells were observed [10-11]. However, to the best of our knowledge, no study has attempted to examine the complex flow structure in the mixing zone at confluences under an ice cover.

The objective of this study is to characterize and compare the flow structure in the mixing zone at a river confluence with and without an ice cover. The field site is a medium-sized discordant-bed confluence (around 40 m wide) between the Mitis and Neigette Rivers, Quebec (Canada).

2. Methodology

2.1. Study site

The confluence of the Mitis and Neigette Rivers [48°31'31.88"N; 68° 7'58.11"O] is located in the Bas-Saint-Laurent region, near Rimouski (approximately 550 km north-east of Montreal, Quebec, Canada). The drainage area of the Mitis River is 1176 km^2 whereas the Neigette River drains an agricultural watershed of 552 km^2, resulting in a sharp colour contrast in the mixing zone due to its higher suspended load. Drone imagery at various flow conditions reveals a highly dynamic mixing zone with very clear KH vortices (Fig. 1A), occupying a maximum width ranging from around 25% of the parent channel width for low discharge ratios Qr (discharge of the tributary (Neigette) divided by that of the main channel (Mitis)) to 50% of the width when Qr is close to unity (Fig. 1B). The confluence was selected because a thick ice cover is present for most of the winter allowing for safe field work. It is also characterized by a marked bed discordance, exceptionally with a deeper tributary than main channel (mean depth of 0.93 m in the Neigette compared to 0.23 m in the Mitis River). Median diameter is 50 and 15 mm in the Mitis and Neigette Rivers, respectively.

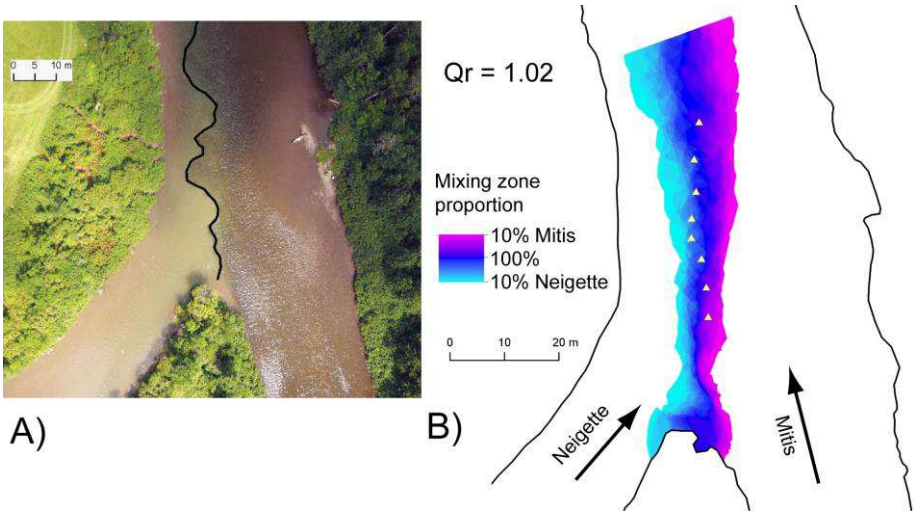

Fig. 1. A) The Mitis Neigette confluence as seen from a drone in the summer, highlighting the marked contrast in colour which allows to delimit the mixing zone (black line); B) Proportion of time in the mixing zone from each tributary when discharge ratio was close to unity (4 December 2015). The yellow triangles correspond to the ADV measurements (Fig. 2A).

2.2. Field measurements

Drone images were taken during ice-free conditions for discharge ratios ranging from 0.09 to 1.02 in order to investigate turbulent structures in the mixing zone. During the winter of 2015, which was characterized by lower-than-average temperature, the ice cover formed in only 14 days, and reached a maximum thickness of 78 cm (43 cm on average) based on measurements made at 146 holes.

Velocity measurements were taken in the mixing zones in ice-covered conditions by digging holes at 8 positions indicated in Fig. 2A. The winter flow conditions, with a discharge of 2.5 and 10.2 m^3/s for the Neigette and Mitis Rivers, respectively (Qr = 0.25) corresponded to typical summer flow conditions.

A Sontek ocean-hydra ADV was used to measure the streamwise (u), lateral (v) and vertical (w) components of velocity at a frequency of 25 Hz. The device was attached to a rod that was lowered from a quadropod (Fig. 2B) to obtain 2-minute long samples at approximately 20 vertical positions. The sampling was done every 2 cm near the bed and near the ice to detect the effect of roughness (see Fig. 2C) on turbulent structures. Two 20-minute samples were also collected at positions T1 and T1A (Fig. 2A).

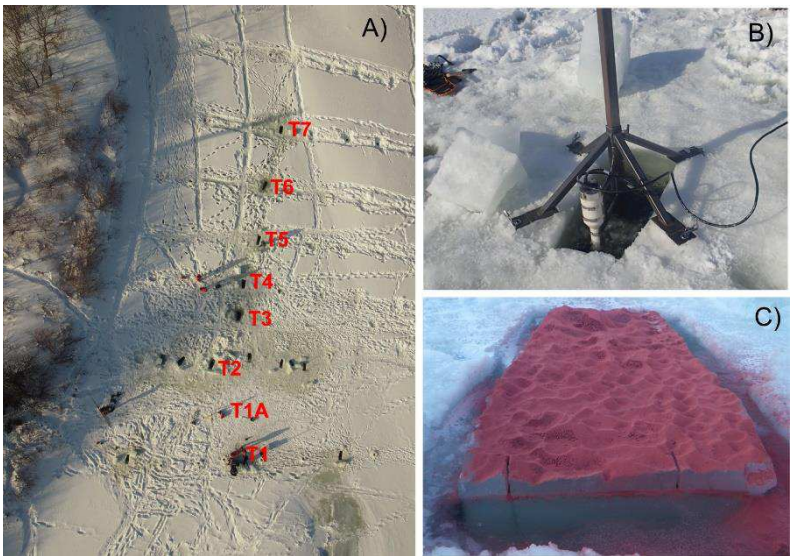

Fig. 2. A) Position of the holes in the ice cover (see Fig. 1B) in the mixing zone where ADV measurements were taken by lowering the instrument from a quadropod (B). C) The roughness under the ice cover at position T7 is revealed using red chalk powder.

3. Results

The mean velocity profiles exhibit the expected opposite logarithmic profiles (Fig. 3), with significant decrease in velocity near the ice cover. Only two examples are presented in Fig. 3, but this pattern was observed at all measured profiles.

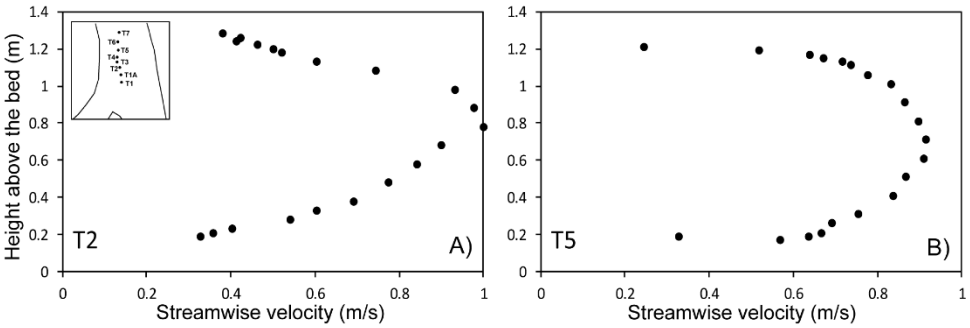

Fig. 3. Mean streamwise velocity profile at positions A) T2 and B) T5.

Instantaneous velocity signals reveal marked differences in turbulent structures in the water column between the near-bed, centre and near-ice positions (Figs. 4, 5). The impact of the ice-cover boundary layer is obvious in both the streamwise and lateral components, with high-frequency large fluctuations in the 25 Hz velocity signals (grey line in Figs 4A, 5A). The instantaneous fluctuations are markedly reduced in the centre of the channel (Figs. 4B, 5B), and increase again close to the bed (Figs. 4C, 5C). Note that only results from position T5 are presented in detail but this pattern was observed at all positions.

A particularly interesting finding of the turbulent signals concerns the lateral velocity component, which is seldom examined in confluence studies. Large-scale structures are

clearly revealed in the 1-second moving average signal (black line in Fig. 5B), with duration ranging between 10 and 20 seconds. With an average velocity of around 0.8 m/s, this corresponds to a structure size of 8 to 16 m. Similar durations were observed through spectral analysis of the 20-minute time series at position T1A, and are thus not specific to position T5. These large-scale lateral structures, however, are not present near the bed or near the ice cover (Fig. 5A,C), suggesting that streamwise and vertical structures (burst/sweep) interfere with the vertically oriented mixing layer structures (KH vortices).

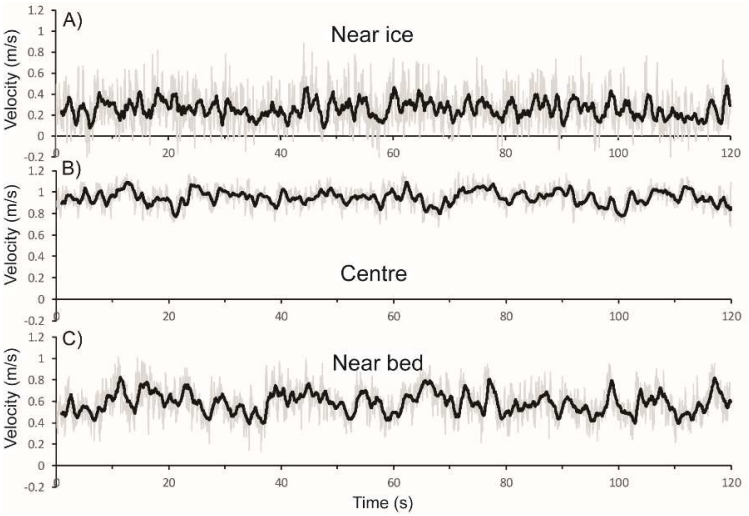

Fig. 4. Time series of instantaneous (grey) and 1-second moving average (black) streamwise velocity at position T5 A) near the ice, B) in the centre of the channel and C) near the bed.

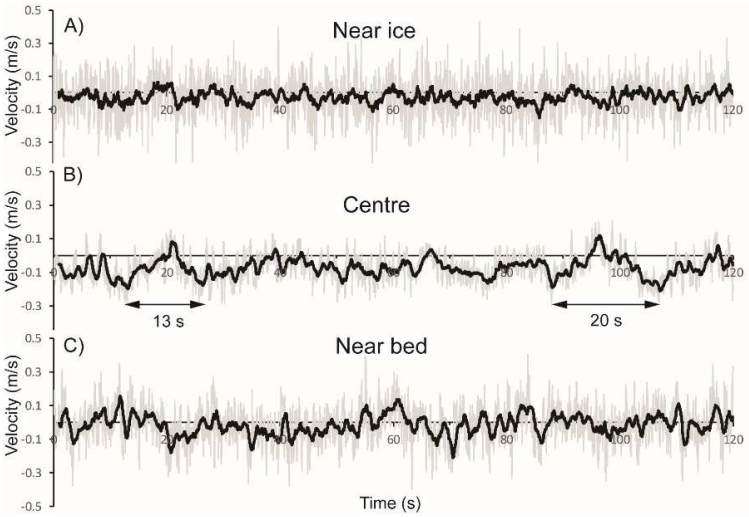

Fig. 5. Time series of instantaneous (grey) and 1-second moving average (black) lateral velocity at position T5 A) near the ice, B) in the centre of the channel and C) near the bed.

There is a strong correlation between the streamwise and lateral turbulent velocity signals, highlighting the presence of large-scale structures located in the centre of the water column

in the mixing zone (Fig. 6). This correlation is consistent with the presence of KH vortices [12], with faster-moving flow structures mainly associated with water movement towards the left bank (black arrows in Fig. 6) and slower-moving structures oriented towards the right bank (grey arrows in Fig. 6). A cross-correlation analysis confirmed this with r_{uv} values (correlation coefficient between the streamwise and lateral component) close to -0.4 in the centre of the water column for all positions. The values of r_{uv} near the bed and near the ice cover remain close to 0, as would be expected in a simple boundary layer with burst/sweep dominant turbulent structures, i.e. streamwise and vertical cross-correlation (r_{uw}) close to -0.4 and 0.4 in the near-bed region and in the near-ice regions, respectively

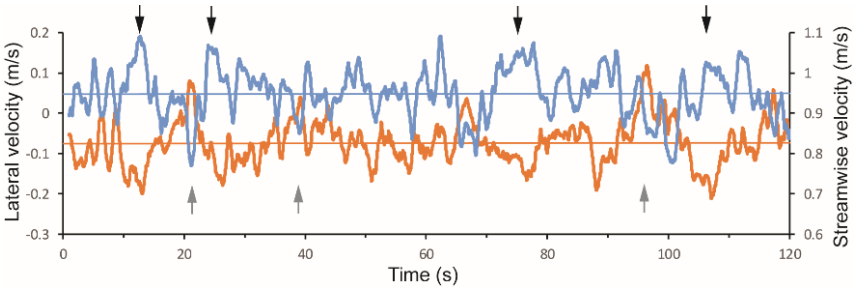

Fig. 6. Streamwise (blue) and lateral (orange) time series (1-second moving average) at position T5 in the centre of the channel. The black arrows on the top highlight faster-moving structures oriented towards the left bank (negative lateral velocity) whereas the grey arrows at the bottom highlight slower-moving structures oriented towards the right bank (positive lateral velocity).

The presence of large-scale KH structures is also revealed by integral time scale analysis at position T5 of the turbulent velocity signal, which, for the streamwise component, increases from 0.10 s near the bed to 0.53 s in the centre down to 0.42 s near the ice. For the lateral component, the changes in integral time scale from the bed to the ice cover are even more marked, i.e. 0.06 s near the bed, 0.90 s in the centre and 0.34 s near the ice cover. This indicates that the size of the mixing layer vortices is reduced in the presence of an ice cover, in contrast to the ice-free situation where the largest KH vortices are observed at the water surface.

4. Conclusions

This field study on confluence mixing processes is novel in many ways, i.e. confluence size, presence of an ice cover, reversed bed discordance (tributary deeper than the main channel) and the detailed analysis of the lateral velocity component which, to the best of our knowledge, has not been thoroughly investigated in mixing zones, with a few recent exceptions of 90° junction laboratory and modelling studies [12,13].

The very good visualization of the mixing zone through difference between the turbid tributary (Neigette) and clearer main channel (Mitis) allowed for an in-depth analysis of mixing layer processes through drone imagery. These video results, not presented here, highlight a marked unsteadiness ("flapping") in the mixing interface position over time for a range of flow conditions. This flapping motion has been attributed in past studies to bimodal oscillations of the streamwise-oriented cells [3]. Here, the dominating structure is clearly KH (vertically-oriented) vortices as observed qualitatively from drone imagery in ice-free conditions, and quantitatively from combined streamwise and lateral velocity turbulent signals under an ice cover. Because the Mitis River is faster than the Neigette River, the

velocity ratio was always different from one in all observed flow conditions, so KH vortices are expected to dominate [3,5]. One of the key findings of this study is that the lateral component is key in interpreting the type of vortical structures present in the mixing zone. More research on lateral velocity fluctuations could indeed help disentangle which dominant structures are present (KH or SOV) in cases where visualization is not as obvious as for the Mitis-Neigette confluence.

The cross-correlation analysis revealed the expected absolute values of 0.4 between the streamwise and vertical components of velocity both close to the bed and close to the ice over, indicating burst/sweep type of structures in the near-bed region and inverted burst/sweep structures in the near-ice region. In the centre of the channel where these turbulent structures vanish, very strong correlation between the streamwise and lateral components of velocity were observed. In ice-free conditions, the size of KH vortices continues to grow towards the surface as they are not affected by the upper boundary layer. This is depicted in a spatio-temporal conceptual model comparing the ice-free and winter conditions in the mixing zone (Fig. 7).

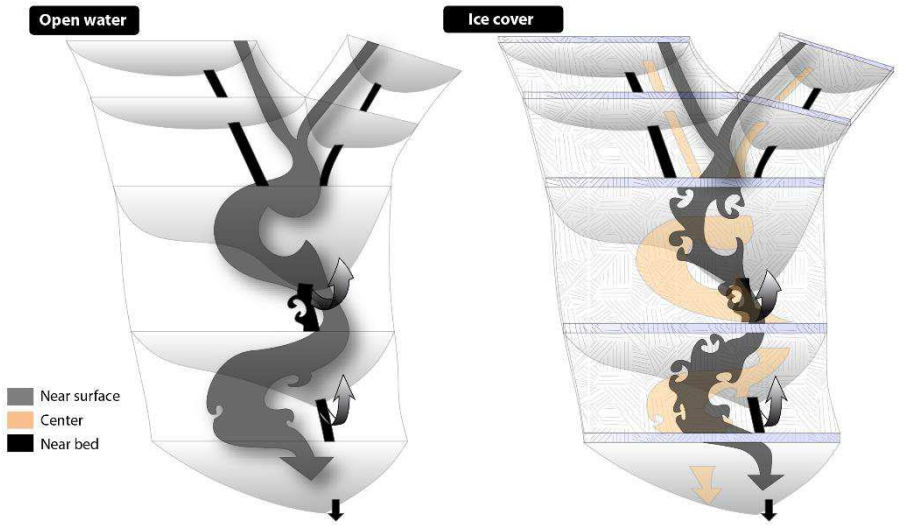

Fig. 7. Conceptual model of vortical structures in the confluence mixing zone under A) ice-free conditions and B) winter conditions.

Future research on confluence dynamics should include more medium-sized field sites with downstream channel width > 30 m, which are presently under-represented in the scientific literature. In these cases, interactions between the mixing zone and the bank zone, as described for example in detail in the numerical simulations of the Kaskaskia and Copper Slough confluence [3], may not play such a major role since the mixing zone is located further away from the bank. Although overall patterns of mean velocity can be useful in explaining flow dynamics, more work on three-dimensional turbulent signals, in particular the lateral component, is also needed to improve our understanding of the flapping motion in the mixing zone as it may have important impacts on sediment transport.

The research was funded by NSERC Discovery grants of T. Buffin-Bélanger and P. Biron and by the Fonds de Recherche Nature et Technologies (FRQNT) scholarship to Nancy Martel.

References

1. J. L. Best, *Recent Developments in Fluvial Sedimentology*, Ethridge, F. G., Flores, R. M., Harvey, M. D. (Eds). SEPM Spec. Publ. **39** (1987)
2. P. M. Biron, J. L. Best, A. G. Roy, J. Hydraul. Eng. **122**, 27-35 (1996)
3. G. M. Constantinescu, S. Miyawaki, B. Rhoads, A. Sukhodolov, J. Geophys. Res. Earth Surface **117**, F04028 (2012)
4. M. Leite Ribeiro, K. Blanckaert, A. G. Roy, A. J. Schleiss, J. Geophys. Res. Earth Surface **117**, F01035 (2012)
5. G. M. Constantinescu, S. Miyawaki, B. Rhoads, A. Sukhodolov, J. Geophys. Res. Earth Surface **119**, 2079-2097 (2014)
6. B. De Serres, A. G. Roy, P. M. Biron, J. L. Best, Geomorphology **26**, 313-335 (1999)
7. C. Boyer, A. G. Roy, J. L. Best, J. Geophys. Res. Earth Surface **111**, F04007 (2006)
8. D. R. Parsons, J. L. Best, S. N. Lane, O. Orfeo, R. J. Hardy, R. Kostaschuk, Earth Surf. Process. Landf. **32**, 155-162 (2007)
9. J. Sui, J. Wang, Y. He, F. Krol. Int. J. Sed. Re. **25**, 39-51 (2010)
10. S. Demers, T. Buffin-Bélanger, A. G. Roy. River Res. Appl. **27**, 1118–1125 (2011)
11. E. Lotsari, E. Kasvi, M. Kämäri, P. Alho. Earth Surf. Process. Landf. **42**, 1195-1212 (2016)
12. S. Yuan, H. Tang, Y. Xiao, X. Qiu, H. Zhang, D. Yu. J. Hydro-Env. Res **12**, 130-147 (2016)
13. L. Schindfessel, S. Creëlle, T. De Mulder. Water **7**, 4724-4751 (2015)